Response of the Lower St. Lawrence Estuary to External Forcing in Winter

G. C. SMITH

Department of Atmospheric and Oceanic Sciences, McGill University, Montreal, Quebec, Canada

F. J. SAUCIER

Institut des Sciences de la Mer, Université du Québec à Rimouski, Rimouski, Quebec, Canada

D. STRAUB

Department of Atmospheric and Oceanic Sciences, McGill University, Montreal, Quebec, Canada

(Manuscript received 7 February 2005, in final form 13 December 2005)

ABSTRACT

Mostly because of a lack of observations, fundamental aspects of the St. Lawrence Estuary's wintertime response to forcing remain poorly understood. The results of a field campaign over the winter of 2002/03 in the estuary are presented. The response of the system to tidal forcing is assessed through the use of harmonic analyses of temperature, salinity, sea level, and current observations. The analyses confirm previous evidence for the presence of semidiurnal internal tides, albeit at greater depths than previously observed for ice-free months. The low-frequency tidal streams were found to be mostly baroclinic in character and to produce an important neap tide intensification of the estuarine circulation. Despite stronger atmospheric momentum forcing in winter, the response is found to be less coherent with the winds than seen in previous studies of ice-free months. The tidal residuals show the cold intermediate layer in the estuary is renewed rapidly (14 days) in late March by the advection of a wedge of near-freezing waters from the Gulf of St. Lawrence. In situ processes appeared to play a lesser role in the renewal of this layer. In particular, significant wintertime deepening of the estuarine surface mixed layer was prevented by surface stability, which remained high throughout the winter. The observations also suggest that the bottom circulation was intensified during winter, with the intrusion in the deep layer of relatively warm Atlantic waters, such that the 3°C isotherm rose from below 150 m to near 60 m.

1. Introduction

The results of a field campaign designed to observe the response of a stratified estuary to atmospheric and tidal forcing in winter are presented. The region of study is the St. Lawrence Estuary, a seasonally ice-covered 200-km-long channel connected to the Atlantic Ocean through the Gulf of St. Lawrence. The estuary can be subdivided into two regions: the shallow (30 m) upper estuary and the deep (>300 m) stratified lower estuary. The circulation in the lower estuary is strongly influenced by Coriolis effects, with the presence of mesoscale phenomena including coastal jets, internal

Corresponding author address: Gregory Smith, Environmental Systems Science Centre, Reading University, 3 Earley Gate, RG6 6AL Reading, United Kingdom.

E-mail: gregory.smith@mail.mcgill.ca

Kelvin waves, baroclinic eddies, and unstable waves (Lie and El-Sabh 1983). Stratification is maintained year-round by the high river runoff (average of 16 000 m³ s⁻¹) (Tee 1989) provided primarily by the St. Lawrence River.

The most prominent bathymetric feature of the lower estuary is the Laurentian Channel, a 300- to 450-m-deep channel running from the shelf break to a 30-m sill. There, strong tidal flood currents lift denser waters from intermediate depths over the sill and allow for important exchanges of heat and salt with the brackish waters of the upper estuary (Gratton et al. 1988). This tidal mixing at the head of the Laurentian Channel drives the ventilation and withdrawal of the deeper layer of warm (5°C) saline (34.5 psu) Atlantic slope water as well as the cold intermediate layer present in the estuary in summer. On the ebb tide, large-amplitude internal waves with vertical excursions of up to

80 m are generated (Forrester 1974) and propagate downstream. A semidiurnal Poincaré internal tide and a diurnal tide of the Kelvin type have been suggested to exist by Forrester (1974). However, whether the properties of these waves are significantly affected by reduced stratification in winter and the presence of sea ice is not known. One focus of this study is thus to determine if, and how, tidal constituents and internal tides in the estuary vary seasonally. The approach will be to perform a harmonic analysis (Foreman 1977) on wintertime current observations from a moored acoustic Doppler current profiler (ADCP).

A second goal of the tidal analysis presented is to investigate the low-frequency tidal response of the estuary as it relates to the baroclinic circulation. Important fortnightly and monthly variations of the estuarine circulation and deep water renewal due to tidal forcing have been demonstrated for other estuaries (Geyer and Cannon 1982; Stacey et al. 1987; LeBlond et al. 1991; Hibiya and LeBlond 1993; Baker and Pond 1995). However, there is some controversy regarding the existence of a low-frequency tidal signal in the currents of the lower St. Lawrence Estuary. Farquharson (1966) suggests that nonlinear frictional effects generate fortnightly current variations in the lower estuary. Mertz et al. (1988) argue that, since the lower estuary is relatively deep (>300 m), such variations would be quite small (1.4 cm s^{-1}) . However, Tee (1989) finds that most of the variance at low frequencies in the lower estuary can be attributed to tidal forcing. We will quantify the amplitude and vertical structure of the MS_f and M_m signal using the aforementioned harmonic analysis.

The response of the estuary to wind forcing will also be examined. Mertz et al. (1988) find that wind forcing dominates the subtidal variability of the lower estuary in the 10–15-day and 40–80-day bands. They conjecture that the lack of coherence at frequencies between these two bands is due to the presence of spatially stationary eddies (El-Sabh et al. 1982) associated with a transverse current around Rimouski. It is not clear how this circulation pattern and the overall response to atmospheric forcing may differ in winter. In section 4, an analysis is presented of the response to wind forcing in terms of the correlation and coherence of observed water mass properties and circulation. One may expect a higher coherence between the currents and winds, given the greater intensity of the latter in winter. However, large ice floes are an effective inhibitor of momentum transfer, acting as a fixed barrier between the atmosphere and ocean by redirecting wind energy into ridging and deformation. On the other hand, free ice floes may amplify the influence of winds by extracting

additional energy from the atmosphere through enhanced drag (Dawson 1901). As the areal ice concentration in the estuary can vary considerably on hourly to interannual time scales (Matheson 1967), the integrated effect of the ice cover on momentum transmission from the atmosphere is unclear.

Despite the strong winds and variable sea ice cover, high surface stability in the lower estuary is thought to be sufficient to inhibit substantial vertical fluxes, and thereby limit winter mixed layer deepening (Ingram 1979). The cold intermediate layer present in the estuary in summer is thus thought to have been transported there, having been formed in the Gulf of St. Lawrence and Labrador Sea (Banks 1966). How the estuary's water-mass properties and structure evolve through winter, however, is not known. A principal goal of this study is thus to provide observations of this evolution and, in particular, of the renewal of the cold intermediate layer. We will begin with a presentation of the observations (section 2b), followed by the tidal analysis (section 3) and study of the response to atmospheric forcing (section 4). We end with a discussion of the subtidal currents and water-mass properties (section 5) and concluding remarks (section 6).

2. Observational methods

a. Mooring details

To study the response of the estuary to winter forcing, observations from three moorings for the winter of 2002/03 will be used. The moorings were located in the northwest gulf (NWG), the lower St. Lawrence Estuary (SLE), and at the head of the Laurentian Channel (HLC) (shown in Fig. 1). Details of the mooring positions and deployment times are shown in Table 1. These observations were obtained as part of a larger field campaign, designed to study the formation and circulation of the intermediate waters in the St. Lawrence Estuary and Gulf of St. Lawrence (Smith et al. 2006).

Mooring NWG consisted of a Seabird SBE19 sampling temperature, conductivity, and pressure at 15-min intervals. The CTD was moored near the western shore at a depth of 73 m, 4 m above the seabed. As flow in the northwest gulf is usually cyclonic, NWG provides observations of the water-mass properties of inflow to the estuary. A CTD of the same type and sampling frequency was used for HLC, where it was moored at a depth of 112 m, 8 m from the seabed. This mooring is located directly adjacent to a 30-m sill where large vertical excursions within the water column due to strong tidal currents and internal waves occur. A CTD moored near bottom at this location thus allows for the moni-

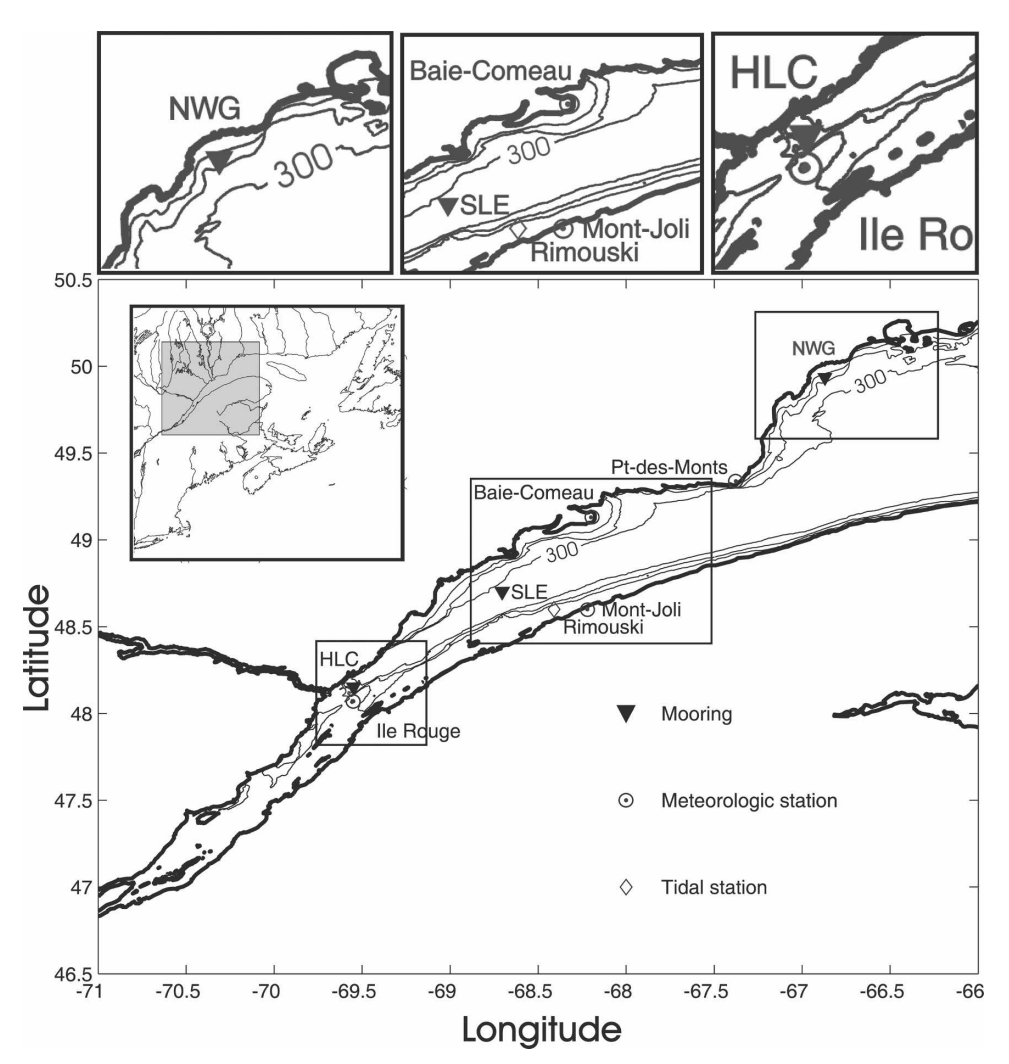


Fig. 1. Bathymetry of the St. Lawrence Estuary. Isobaths are shown for 100, 200, and 300 m. Note the deep (300 m) channel that runs from the mouth to a 30-m sill at the head of the Laurentian Channel. The position of the three moorings (HLC, SLE, and NWG) is indicated. An enlargement of the region of each mooring is also shown.

toring of a relatively large fraction of the water column. Additionally, it serves as a measure of water-mass properties at the end of the Laurentian Channel where strong mixing occurs.

The central mooring of this study is SLE. Its instrumentation was designed to provide observations of the currents as well as the evolution of the thermal structure of the upper portion of the water column throughout the winter. A 2.5-m spatial resolution was obtained using two 25-m Aanderaa thermistor strings with 10 equally spaced thermistors moored at depths of 30–55 m and 60–85 m. Three Vemco Minilog 12 thermistors were attached to the mooring line at depths of 25.0, 27.5, and 57.5 m, thereby completing the vertical coverage. However, owing to faulty instrumentation, significant gaps exist in the time series from the deeper

of the two thermistor chains. Minilog thermistors were also located every 10 m from 90- to 200-m depth, with the exception of 120 m. There, a 300-kHz Workhorse Sentinel ADCP was mounted with an upward-pointing

TABLE 1. Summary of the mooring details. The location of these moorings is also shown in Fig. 1. SLE had a vertical array of thermistors as well as an upward-pointing ADCP. HLC and NWG both employed a single CTD, moored near the seabed.

	Lat (°N)	Lon (°W)	Depth (m)	Date deployed (2002)	Date retrieved (2003)
SLE	48°42.17′	68°42.29′	342	7 Nov	17 Apr
HLC	48°9.00′	69°33.00′	120	7 Nov	7 Jun
NWG	49°56.20′	66°53.20′	77	27 Oct	18 Apr

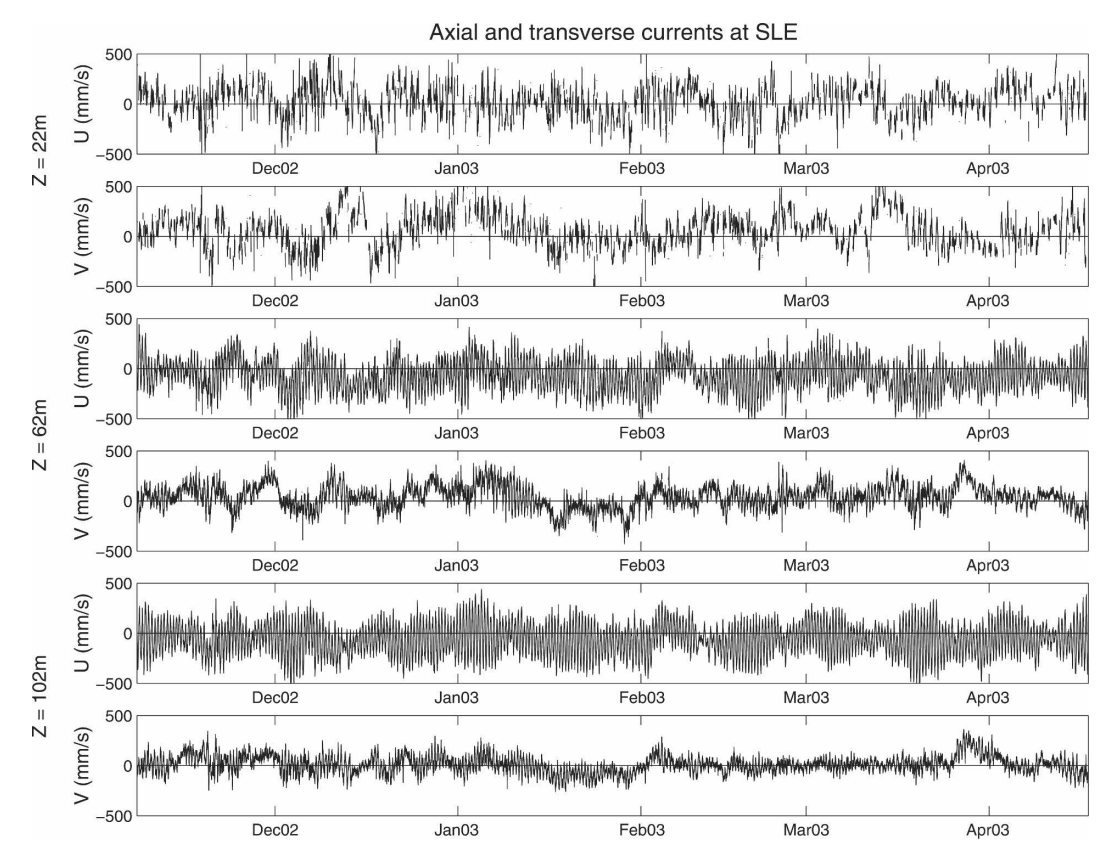


Fig. 2. Axial (U) and transverse (V) components of the observed currents in the lower St. Lawrence Estuary (mooring SLE) are shown for three depths (22, 62, and 102 m). The observations span the top 120 m of the water column with a 2.5-m resolution. Positive axial and transverse directions point downstream (northeast) and northwestward, respectively. Note that roughly 40% of the data in the 22-m time series have been omitted (see text).

orientation. The Minilogs sampled temperature at 30-min intervals, whereas the thermistor chains sampled every hour. The ADCP provided velocity measurements in 2.5-m bins from 112 to 9.5 m. Two criteria were used to remove erroneous velocity data: a maximum threshold value of 2 m s⁻¹ and a minimum 50-count average correlation value among the four heads of the ADCP. This removed 40% of the observations of the upper 40 m of the water column and had little effect on the deeper waters.

b. Data description

1) Mooring site SLE: St. Lawrence Estuary

The along- and cross-channel currents at 22, 62, and 102 m are shown in Fig. 2. Here, positive along-channel currents correspond to downstream flow (57°) and positive cross-channel currents to flow northwestward (327°) . A strong tidal influence can be clearly seen in the currents, especially in the along-channel direction at depths of 62 and 102 m. Strong low-frequency vari-

ability occurs throughout the time series, with $40 \, \mathrm{cm \ s^{-1}}$ along-channel currents occurring in both upstream and downstream directions. The cross-channel currents also show large-amplitude low-frequency variations on the order of $40 \, \mathrm{cm \ s^{-1}}$.

Observations of temperature from both Minilog data recorders and thermistor chains at SLE are shown in Fig. 3. Important oscillations are present with periods from days to weeks at all depths. A three-layer structure is evident throughout November with a cold intermediate layer persisting below the seasonal thermocline. The formation of near-freezing surface waters begins around late December. Throughout winter, the surface mixed layer remains shallow, reaching a maximum thickness of 60 m by mid-March. A gradual shoaling of the 3°C isotherm occurs over winter, reaching a depth of 60 m for a brief period in February. In April there is a rapid recession of this isotherm with the arrival of a layer of near-freezing waters at depths of 40-100 m. Improving our understanding of how this water mass is renewed in the estuary is one of the primary

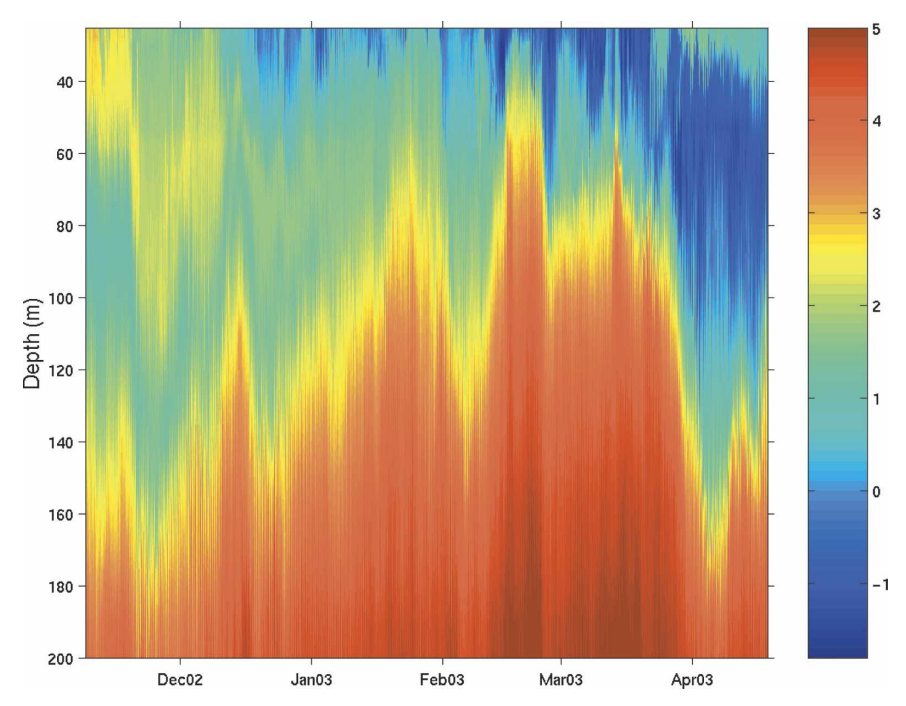


Fig. 3. Observations of temperature (°C) in the lower St. Lawrence Estuary (mooring SLE). Instruments are spaced vertically every 2.5 m from 25 to 85 m, and every 10 m from 90 to 200 m. Gaps exist in the data from thermistors moored between 60 and 85 m.

goals of this study. Over the spring-autumn period this layer undergoes a gradual warming from both above and below. Remnants of the previous year's cold intermediate layer can be seen in November in Fig. 3.

2) MOORING SITE HLC: HEAD OF THE LAURENTIAN CHANNEL

Temperature and salinity observations from mooring HLC (Fig. 4) show strong diurnal and semidiurnal variability. This is due in part to the interaction of the intense tidal currents (Farquharson 1970) and the 30-m sill located 2.5 km directly upstream from the mooring site. Large-amplitude internal waves and tides have been shown to exist in this region (Forrester 1974). Significant synoptic-scale variability is present in the temperature and salinity, with an amplitude greater than 2°C and 2 psu. A low-frequency seasonal signal is also apparent, with a gradual increase in temperature and salinity throughout winter and a subsequent decrease in April, similar to that seen for SLE (Fig. 3).

3) Mooring site NWG: Northwest gulf

The CTD data from NWG is shown in Fig. 5. High-frequency variability, possibly associated with tidal forcing, the passage of storms, or internal wave activity, is present throughout the time series. Significant seasonal variability exists in both salinity and temperature

observations. Throughout November, a warming and freshening due likely to the downward diffusion of heat and freshwater from the summer mixed layer occurs. A month-long period of cooling follows until early January. This cooling is accompanied by significant salinity fluctuations (~1 psu) and a drift toward higher values. An upward trend in the maximum temperature can be observed from January to mid-March, interspersed

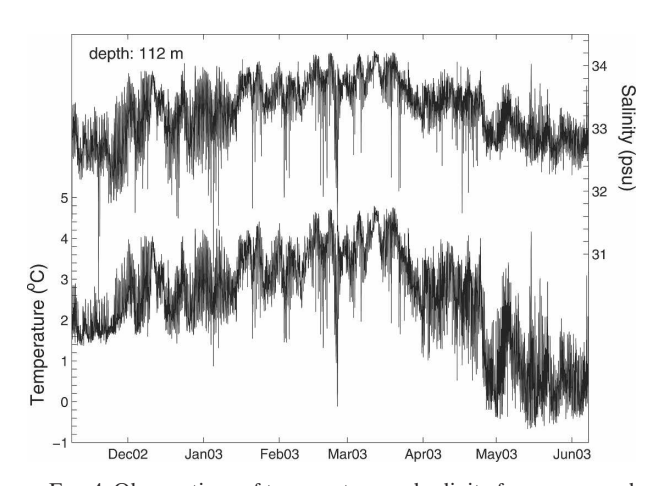


FIG. 4. Observations of temperature and salinity from a moored CTD at the head of the Laurentian Channel (HLC) over the winter 2002/03 (see Fig. 1 and Table 1 for location). The CTD was moored at a depth of 112 m, 8 m from the seabed.

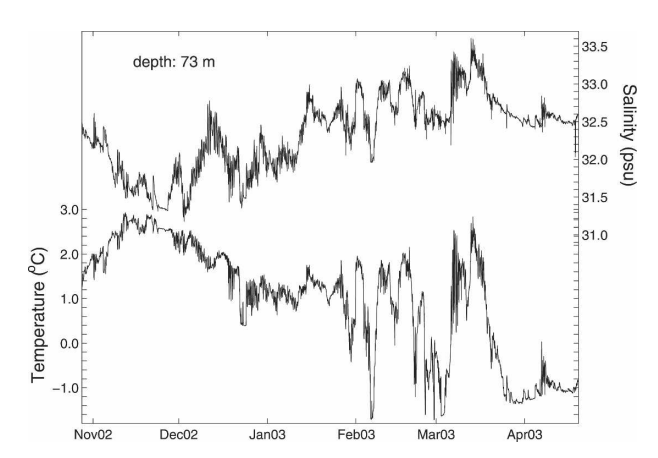


Fig. 5. Observations of temperature and salinity from a moored CTD in the northwest gulf (NWG) over the winter 2002/03 (see Fig. 1 and Table 1 for location). The CTD was moored at a depth of 73 m, 4 m above the seabed.

with short periods of colder and less saline water. Given the location of this mooring in a region of steep bathymetry near shore, the intermittent appearance of these colder waters is most likely associated with downwelling events. After 26 March, the temperature remains near -1.2° C for the remainder of the time series. This transition in spring, common to all three moorings, is discussed further in section 5b in terms of the renewal of the cold intermediate layer.

It should be noted that the cooling and freshening in April is not density compensating and is associated with a reduction in potential density of 0.4 kg m⁻³. This reduction suggests that a change in the local circulation in the northwest gulf in spring may have occurred (Smith et al. 2006). For example, the circulation in the northwest gulf is usually dominated by the presence of a barotropic cyclonic gyre. This circulation pattern is associated with a doming of the isopycnals in the center of the gyre and a deepening of the isopycnals near shore. Thus, a change in this circulation pattern could be responsible for the observed reduction in potential density observed in spring at NWG.

4) SUPPLEMENTARY DATA

Additional observations have been included in order to investigate the estuary's response to atmospheric momentum forcing as well as to contextualize the external forcing. Data from three meteorological stations (Ile Rouge, Mont-Joli, and Pointe-des-Monts) will be used to address the response to wind forcing. Observations from a tide station have been included to provide information on the surface tide and water-mass conditions.

Observations of temperature, pressure, and winds for

winter 2002/03 from the meteorological station at Mont-Joli are shown in Fig. 6. The mean surface air temperature at Mont-Joli in winter (1 December–1 April) was -9.3° C, and fell below -20° C seven times, once for nearly a week. Rapid changes occur in atmospheric pressure and winds associated with the passage of winter storms. Indeed, at Mont-Joli (Fig. 6) the pressure drops to near 98 kPa on six occasions. The occurrence of periods of low pressure ends in late March with the spring onset of positive surface air temperatures.

Water level, sea surface salinity, and temperature from a tide gauge station at Rimouski are shown in Fig. 7. The tidal range at Rimouski is roughly 2.5 m, with significant low-frequency variations. A strong fortnightly and monthly signal is present in the sea surface salinity, with maximum salinities occurring roughly in phase with neap tide. The sea surface temperature reaches the freezing point in December and remains near freezing until the end of March. Accordingly, sea ice in the lower estuary begins forming in December and most melting had been accomplished by late March. Near-complete ice concentrations existed for most of January and February of 2003 with ice thicknesses generally in the range of 5–10 cm. However, the sea ice cover exhibited a high degree of variability throughout winter, with rapid shifts from nearly complete concentrations to open water in a matter of hours.

The largest contributor of freshwater runoff into the estuary is the St. Lawrence River (80%), which generally reaches its annual maximum in May with a value of 23 600 m³ s⁻¹ (Koutitonsky and Bugden 1991). The runoff from this river in 2003 was quite low, having a maximum in May of only 12 400 m³ s⁻¹. Moreover, the runoff in February (the annual minimum) was only 8700 m³ s⁻¹, as compared with a climatological value of 13 300 m³ s⁻¹. The freshwater outflow from the St. Lawrence River in 2003 was the lowest observed since 1965.

3. Tidal analysis

In this section we will present results of a harmonic analysis (Foreman 1977) of ADCP and thermistor observations. Particular attention is paid to internal tides and the low-frequency modulation of the estuarine circulation and thermal structure. For the currents, the tidal ellipse parameters for each constituent were converted into values for the along- and cross-channel amplitude and phase.

a. Semidiurnal and diurnal tidal currents

Values for the amplitude and phase of the seven most significant tidal constituents at three depths are shown

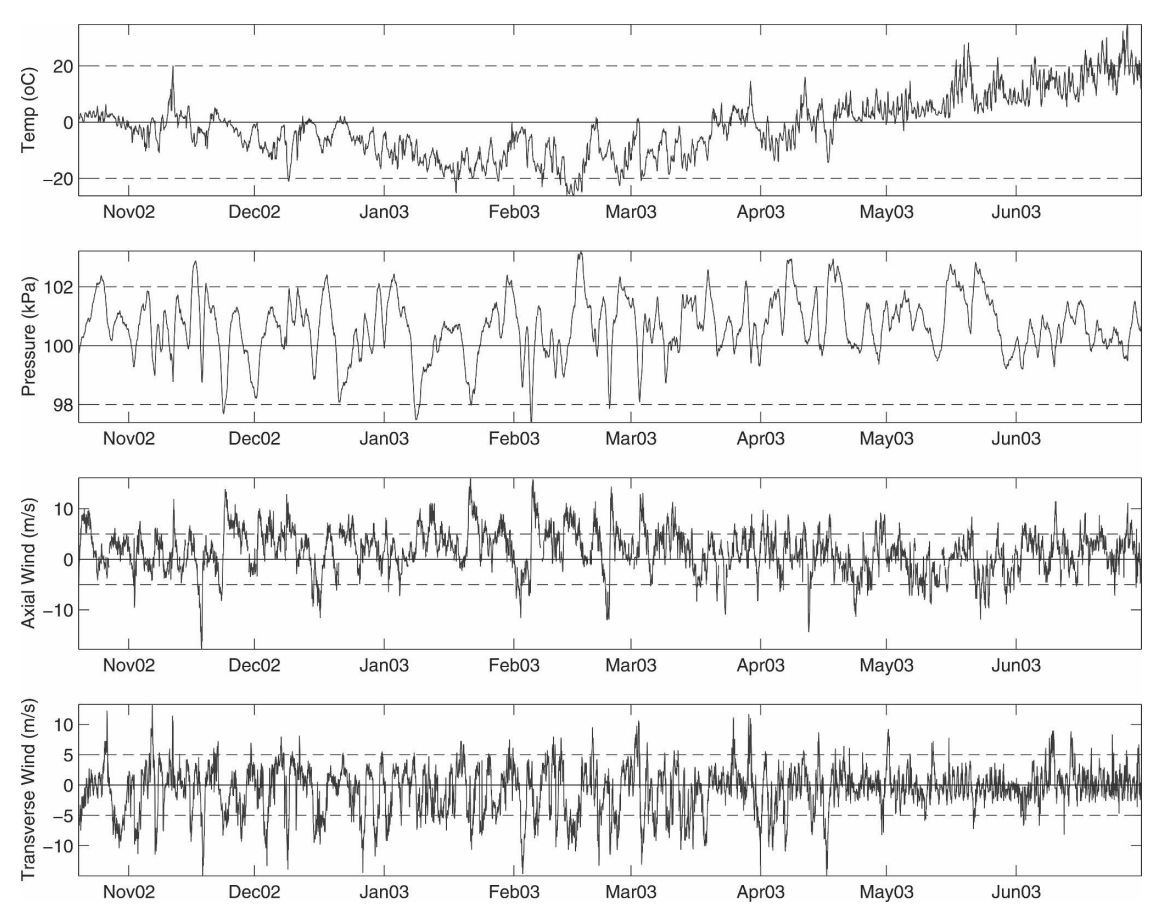


Fig. 6. Observations of atmospheric temperature, pressure, and winds at Mont-Joli, Québec (see Fig. 1 for location). Guidelines have been plotted for the temperature at $\pm 20^{\circ}$ C. Pressure guidelines have been plotted at 100 kPa (solid) as well as 102 and 98 kPa (dotted). For the winds, guidelines have been plotted for values of zero (solid) and $\pm 5 \text{ m s}^{-1}$ (dotted).

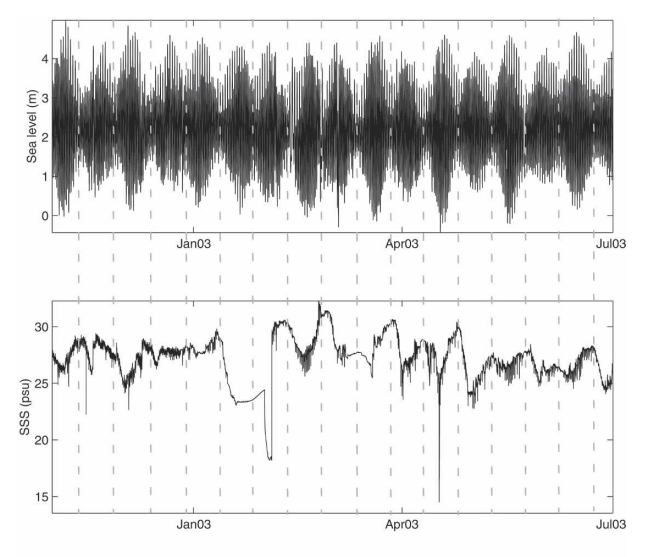
in Table 2. The M_2 amplitude at 22 m (9 cm s⁻¹) is smaller than the values shown in Table I of Forrester (1974) (17–30 cm s⁻¹ at depths of 13–18 m) for several moorings located within 20 km of SLE. This strong decrease in amplitude may be due to frictional damping from sea ice (Godin 1972). For the M_2 phase, the values at 22 m for SLE lead those of Forrester (1974) by 26°–50°. The advance of the phase in winter is also consistent with increased surface drag due to sea ice. This interaction of the tidal currents and sea ice is consistent with previous findings of a semidiurnal and diurnal tidal signal in ice velocities (Johannesson et al. 1968).

We will now examine the semidiurnal and diurnal baroclinic tidal currents. The observed tidal stream can be considered as being the sum of a barotropic tidal current towing to the surface tide and a baroclinic tidal current resulting from internal tides. Here, the barotropic tidal stream was calculated by assuming that the tidal statistics for all depths greater than those observed (120 m) were equal to the value at the maximum ob-

served depth. The barotropic currents obtained using this method agree well with the "continuity streams" of Forrester (1972).

The M_2 baroclinic tidal stream is shown in Fig. 8. These observations compare well with the findings of Forrester (1974) and Saucier and Chassé (2000). The presence of a 180° phase shift and the strong surface intensification of the along-channel component are consistent with the existence an internal M_2 tide as suggested by Forrester (1974). However, the calculation of Forrester predicts the upper phase shift to be at 40 m, whereas here it is found at 80 m. This is most likely representative of seasonal changes in stratification. Stratification in winter is reduced because of low freshwater runoff, increased mixing from high surface stresses, and the destabilizing effect of sea ice formation. A deepening of the 180° phase shift is consistent with the presence of a thicker surface mixed layer in winter than in the summer period studied by Forrester (1974).

Further evidence for seasonal variations in the inter-



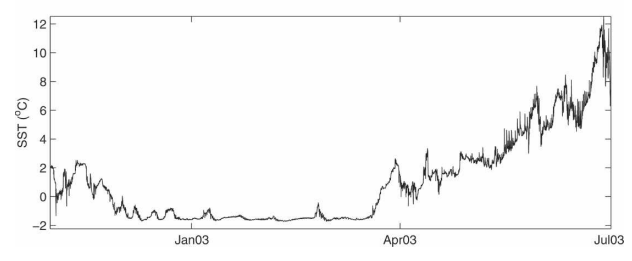


FIG. 7. Observations of water level, sea surface salinity (SSS), and temperature (SST) from a tide gauge station at Rimouski, Québec (see Fig. 1 for location). Vertical lines have been drawn to highlight the relationship between fortnightly tides and salinity variations

nal tides can be found in the structure of the S_2 and N_2 tides (not shown). As found for M_2 , the S_2 and N_2 tides have a 180° phase shift at greater depths (100 and 115 m, respectively) than found previously. A 180° phase

shift occurs for the O_1 tide around 45 m (not shown), consistent with the findings of Forrester (1974) that there is a diurnal internal tide. The depth of this phase shift does not differ significantly from the value of 40 m found by Forrester (1974).

b. Fortnightly and monthly tidal currents

Table 2 shows the amplitude and phase of the fortnightly (MS_f) and monthly (M_m) tides. Significant amplitudes are found for both components, with values of comparable magnitude to the semidiurnal and diurnal tides. Augmented values of the amplitude of these tides is often attributed (e.g., Stacey et al. 1987) to the transfer of energy into these frequencies by nonlinearities in the system (Godin 1972). For example, a nonlinear interaction between M_2 and S_2 could transfer energy into their beat frequency, the MS_f frequency, which corresponds to a period of 14.77 days. Similarly, energy could be fed into the M_m frequency (having a period of 27.55 days) through a nonlinear interaction of M_2 and N_2 . In the relatively shallow St. Lawrence River, LeBlond (1989) attributes the generation of an MS_f sea level signal to quadratic friction. However, as the channel deepens in the lower estuary, friction becomes less significant and the MS_f signal should weaken. Indeed, LeBlond (1989) and Mertz et al. (1988) both conclude that MS_f variations in the lower St. Lawrence estuary are not readily detectable in short records. Mertz et al. (1988) suggest that the amplitude of MS_f variations are on the order of 1.4 cm s⁻¹, whereas we find a larger signal (near-surface axial amplitude of 6.7 cm s^{-1}).

The barotropic and baroclinic amplitude and phase for the axial component of the MS_f tide are shown in Fig. 8. The MS_f tide has stronger baroclinic currents

TABLE 2. Summary of the harmonic analysis of current observations at SLE. The main tidal constituents are shown for both axial and transverse directions at three depths (22, 63, and 102 m). The amplitude (u) and phase (ϕ) are in millimeters per second and degrees UTC, respectively.

			Axial			Transverse		
SLE		22 m	62 m	102 m	22 m	62 m	102 m	
M_2	и	93 ± 3	145 ± 2	191 ± 2	33 ± 6	3 ± 3	33 ± 2	
-	ϕ	326 ± 3	317 ± 1	319 ± 1	46 ± 8	100 ± 40	258 ± 4	
S_2	и	28.7 ± 3	40 ± 2	55 ± 2	6 ± 6	12 ± 4	10 ± 2	
	ϕ	356 ± 2	0 ± 2	3 ± 2	109 ± 37	73 ± 14	18 ± 8	
N_2	и	29 ± 2	25 ± 3	43 ± 2	13 ± 7	10 ± 4	12 ± 2	
	φ	298 ± 20	315 ± 7	284 ± 3	29 ± 41	342 ± 22	183 ± 12	
K_1	u	16 ± 3	15 ± 2	18 ± 1	4 ± 4	2 ± 3	2 ± 2	
	ϕ	288 ± 12	8 ± 3	32 ± 5	232 ± 43	242 ± 98	137 ± 103	
O_1	и	19 ± 4	9 ± 3	13 ± 1	33 ± 3	5 ± 3	2 ± 2	
	ϕ	34 ± 20	328 ± 17	9 ± 8	318 ± 12	162 ± 30	131 ± 103	
MS_f	и	67 ± 4	29 ± 4	9 ± 4	68 ± 7	29 ± 3	13 ± 2	
	ϕ	135 ± 89	106 ± 15	117 ± 28	229 ± 16	228 ± 16	239 ± 20	
M_m	и	35 ± 3	26 ± 3	22 ± 2	21 ± 6	30 ± 3	25 ± 2	
	φ	196 ± 8	169 ± 9	159 ± 6	263 ± 24	128 ± 9	138 ± 6	

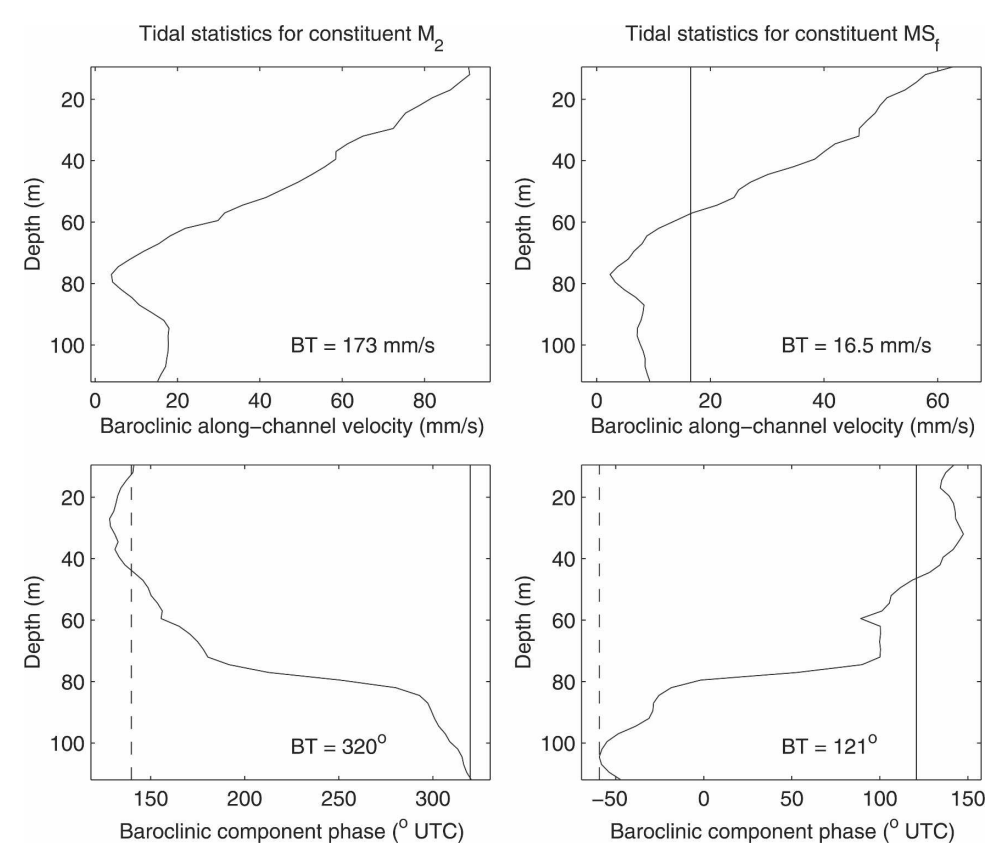


Fig. 8. Vertical dependence of the baroclinic tidal currents for the (left) M_2 and (right) MS_f tides at SLE. The (top) amplitude and (bottom) phase for each tidal component are shown. Solid guidelines indicate the amplitude and phase for the barotropic currents. The dashed guidelines show a 180° phase difference from the barotropic value.

above 60 m for both axial and transverse (not shown) components. A 180° phase shift in both components occurs around 80 m. Since the baroclinic MS_f is in phase with the barotropic tide above 80 m, the estuarine circulation will be enhanced during the barotropic MS_f ebb tide. The behavior of the M_m tide (not shown) is similar to that of MS_f . There exists a 180° phase shift, although it occurs deeper for M_m (105 m). The M_m axial baroclinic amplitude is weaker than that seen for the MS_f tide [barotropic and baroclinic components (at 22 m) have amplitudes of 21 and 34 mm s⁻¹, respectively]. However, the surface intensification and in-phase relationship with the barotropic component above the phase shift remain the same.

Previous studies (e.g., Hibiya and LeBlond 1993) have shown that an enhancement of the fortnightly baroclinic flow may be induced by tidal mixing variations. Owing to stronger tidal currents and shear, the spring tide (or MS_f maximum) is usually associated with an increase in the mixing of momentum and mass. It is possible that this additional mixing acts to diffuse momentum sufficiently to increase the drag between in-

flowing and outflowing layers, thereby reducing the estuarine circulation during spring tide (Geyer and Cannon 1982). The response of the low-frequency tides found here is consistent with this theory. However, another possibility is that fortnightly variations in sea level in the St. Lawrence River may cause significant fluctuations in freshwater discharge, and thus downstream stratification (Koutitonsky and Bugden 1991). Evidence of this is present in the strong fortnightly and monthly variability in the surface salinity in the lower estuary (Fig. 7), with the highest salinities occurring roughly in phase with neap tide.

c. Tidal temperature fluctuations

A harmonic analysis was also performed on the 34 thermistors at SLE. The tidal statistics for the most prominent constituents (M_m , MS_f , and M_2) for three depths are summarized in Table 3. In contrast to the tidal currents, the fraction of variance predicted by the harmonic analysis of temperature observations is quite low. In fact, the maximum explained variance is only 16% and occurs at roughly 80 m. It is interesting that

TABLE 3. Summary of the harmonic analysis on SLE thermistor data. Values are shown for the three most significant constituents
for three depths. For each depth, the columns show the amplitude T (°C) and phase ϕ (°UTC).

	25 m		80 m		200 m	
SLE	T	φ	T	φ	\overline{T}	ϕ
M_m	0.18 ± 0.03	120 ± 10	0.53 ± 0.03	327± 3	0.04 ± 0.01	34±14
MS_f	0.10 ± 0.03	156 ± 20	0.21 ± 0.03	81± 9	0.04 ± 0.01	254±14
M_2	0.08 ± 0.03	235 ± 24	0.05 ± 0.03	217 ± 35	0.14 ± 0.01	195± 4

it is the low-frequency tides that have the greatest tidal amplitudes. The M_m tide is most significant, having an amplitude of 0.5° C, with the MS_f tide having a maximum amplitude of 0.25° C, both of which occur near 80 m.

The MS_f tide also exhibits a 180° phase change (Fig. 9) that may be attributable to fortnightly mixing variations. Because the deeper waters in the estuary are warmer in winter, increased mixing at spring tide induces an upward heat flux. This results in a warming at shallow depths and cooling below, such that neap–spring temperature variations with depth are out of phase.

4. Analysis of atmospheric forcing

It is expected that the response of the estuary to atmospheric momentum forcing in winter is somewhat different to that in other seasons. For example, the presence of sea ice may act as a nonlinear filter on the transfer of momentum, such that surface stresses could be either reduced or enhanced depending on ice characteristics. Moreover, the erosion of the highly stratified estuarine surface layer in winter could affect the baroclinicity of the response. In this section, we begin with a presentation of results of the correlation and coherence of de-tided observations at SLE with atmospheric winds. The response at moorings HLC and NWG will then be shown.

a. Wind forcing at SLE

The correlation between along- and cross-channel winds and the detided residual current from SLE was calculated using the winds at Ile Rouge for the along-

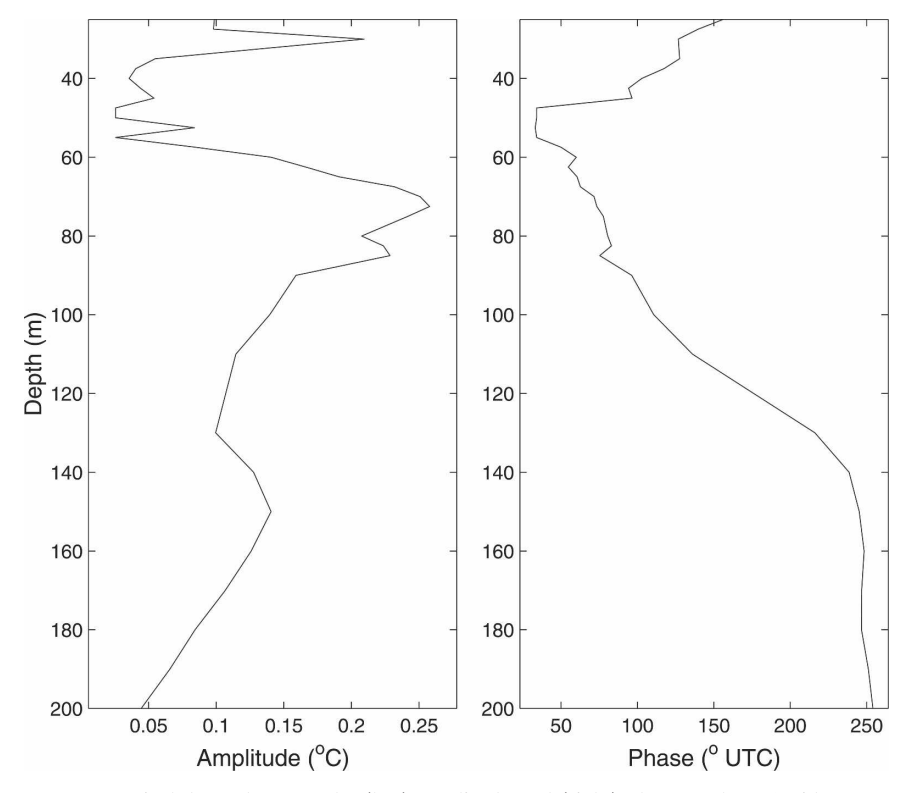


Fig. 9. Vertical dependence of the (left) amplitude and (right) phase of the MS_f tide from thermistor observations at SLE.

channel wind and the Mont-Joli winds for the crosschannel component. These wind stations were chosen since they best represent the given wind component at SLE. The correlations were also calculated using observations from other stations in the region, and the results did not differ significantly. The winds were lowpass filtered using an $\Omega_{24}\Omega_{25}$ moving-window Godin filter (Godin 1972) (half-power point at 67 h) and were decimated (subsampled) to daily values. The residual current was calculated as the difference between the observed currents (see Fig. 2) and the predicted tidal streams (see section 3). The residual currents were similarly low-pass filtered and decimated to daily values. Only correlations with axial currents will be presented here since the correlation of the transverse currents with either wind component showed no statistical significance.

The correlation of along- and cross-channel winds and axial currents is shown in Fig. 10. The 95% significance limits are shown for 80 effective degrees of freedom. A significant positive correlation for the along-channel winds is present in the upper 20 m of the water column for a lag of 2 days. Below 20 m, a small negative correlation exists at longer lag times (6–7 days). A similar, although stronger, response was noted by Mertz et al. (1988), using summertime observations at the mouth of the estuary. They find a positive correlation with the along-channel wind near shore at short lags and a negative correlation in deeper waters at longer lag times.

Significant values are only found for the upper 20 m of the water column for the correlation between the cross-channel wind and the axial currents (Fig. 10). The general response suggests a near-surface (0–60 m) positive correlation at short lags and a negative correlation at depth for longer lag times. However, the low correlation values of both along- and cross-channel winds inhibit a clear understanding of the response.

Moreover, the along-channel winds and currents only show significant coherence squared in the 5–7-day band for near-surface currents (Fig. 11). Similarly, the cross-channel winds and along-channel currents show insignificant coherence squared for frequencies containing the most variance. The limited values of the coherence squared obtained here are in contrast to previous studies (El-Sabh et al. 1982; Mertz et al. 1988; Tee 1989) in ice-free months, which show significant coherence in the 10–15-day band.

b. Wind-forced response at HLC and NWG

The tidal residual time series of temperature, salinity, and sea level (pressure) at both HLC and NWG were filtered and decimated as described previously for the observations at SLE. Significant variance is present in

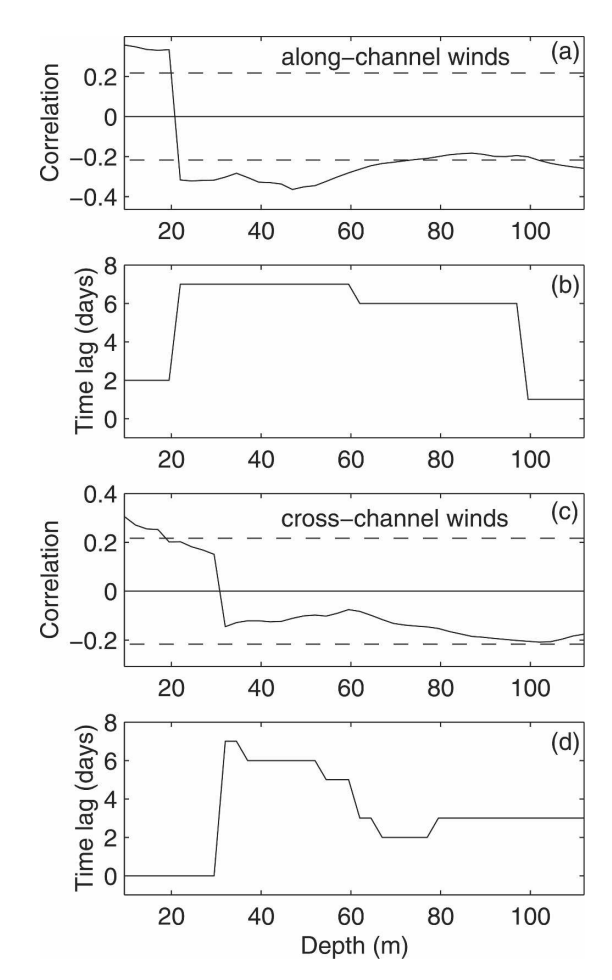


Fig. 10. Amplitude and time lag of maximum correlation between the along- and cross-channel wind and axial residual currents at SLE. (a), (b) The Ile Rouge wind data was used for the along-channel winds and the (c), (d) Mont-Joli wind data for the cross-channel winds.

both the 3–18-day band as well as at low frequencies (not shown) with a particularly large peak at 40 days. The salinity, temperature, and potential density all show significant coherence with along-channel winds at 3.6 days (Fig. 12). Although the coherence squared is significant with respect to the 95% level (using 21 degrees of freedom), the values remains relatively low. Similarly, the coherence with cross-channel winds shows small but significant peaks in the 2–3-day range (not shown). The sea level data (derived from pressure observations) also show significant negative correlation values (-0.5) with the along-channel winds at a lag time of 1 day (not shown).

The power spectral density for the temperature, salinity, and potential density from NWG (not shown) shows a dominant peak at roughly 8.7 days. This is consistent with the passage of coastally trapped shelf waves created by the intense winter winds along the

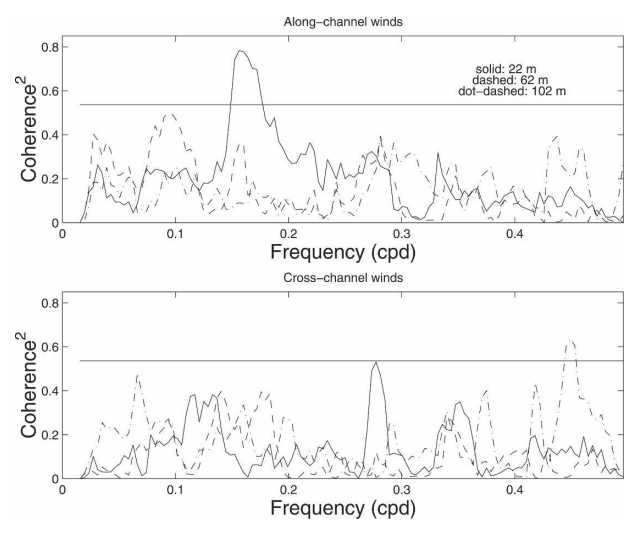


Fig. 11. Coherence squared and phase of the axial currents with (top) along-channel winds and (bottom) cross-channel winds. Values were obtained using a Daniell filter with n=11. The 95% significance level is shown for 22 degrees of freedom. The equivalent bandwidth is 0.07 cpd.

north shore of the Gulf of St. Lawrence. The significant coherence of the winds with temperature, salinity, and potential density near this frequency (Fig. 13) suggests that wind-forced shelf waves may be present in the region. Moreover, the sea level is significantly correlated with both along- and cross-channel winds (-0.38 and -0.5, respectively). Owing to the curvature of the coastline, the cross-channel winds may be considered as a proxy for along-channel winds on the north shore. Given that shelf waves propagate with the coast to their right, shelf waves found at NWG were most likely generated along the north shore.

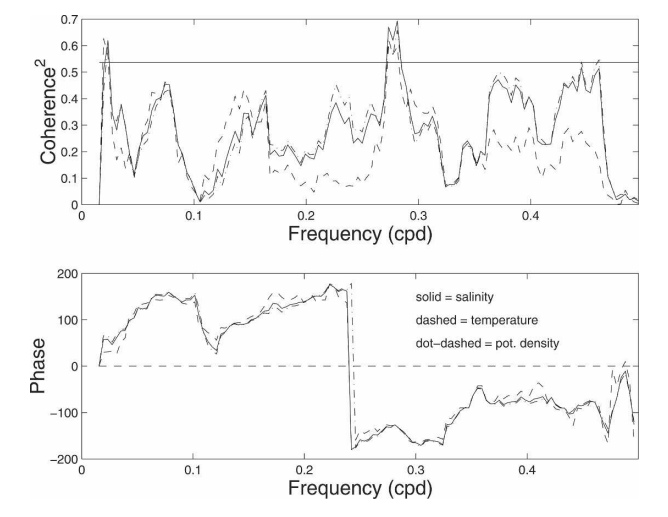


Fig. 12. As in Fig. 11 but of the along-channel winds at Ile Rouge and HLC data.

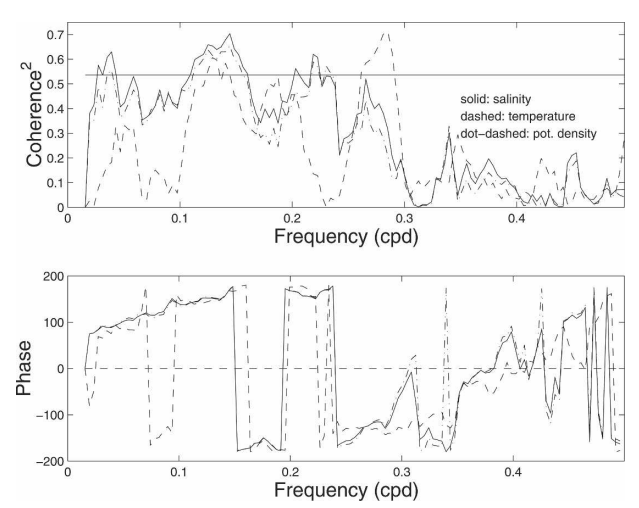


Fig. 13. As in Fig. 12 but of the along-channel winds at Pointe-des-Monts and NWG data.

5. Discussion of subtidal fields

a. Subtidal currents at SLE

1) Axial currents

The axial residual currents (Figs. 14 and 15) are consistent with a two-dimensional estuarine circulation with surface outflow and inflow at depth. Despite the reduction in stratification in winter and the increase in surface momentum forcing, the surface outflow remains quite shallow (30 m). A number of strong reversals at depth occur throughout the period of observation, with outflowing waters having speeds of up to 10 cm s⁻¹. For the second half of March the flow below 40 m was generally inward and relatively intense (10 cm s⁻¹). It is during this period that the cold intermediate layer was renewed (Fig. 3). Although a small significant correlation was found between the axial currents and winds, the low coherence values indicate that the portion of shared variance is relatively small. This lack of a clear response suggests that the renewal of the cold intermediate layer was not simply due to local atmospheric forcing.

2) Transverse currents

The mean near-surface transverse currents show larger values than the axial component (Figs. 14 and 16). The northwestward cross-channel transport occurs over a greater range of depths as well (0–60 m). The relatively large mean value of the transverse current suggests that it may play a more dominant role in the wintertime estuarine circulation than the axial component. The standard deviation of this flow is also much larger than that of the axial current.

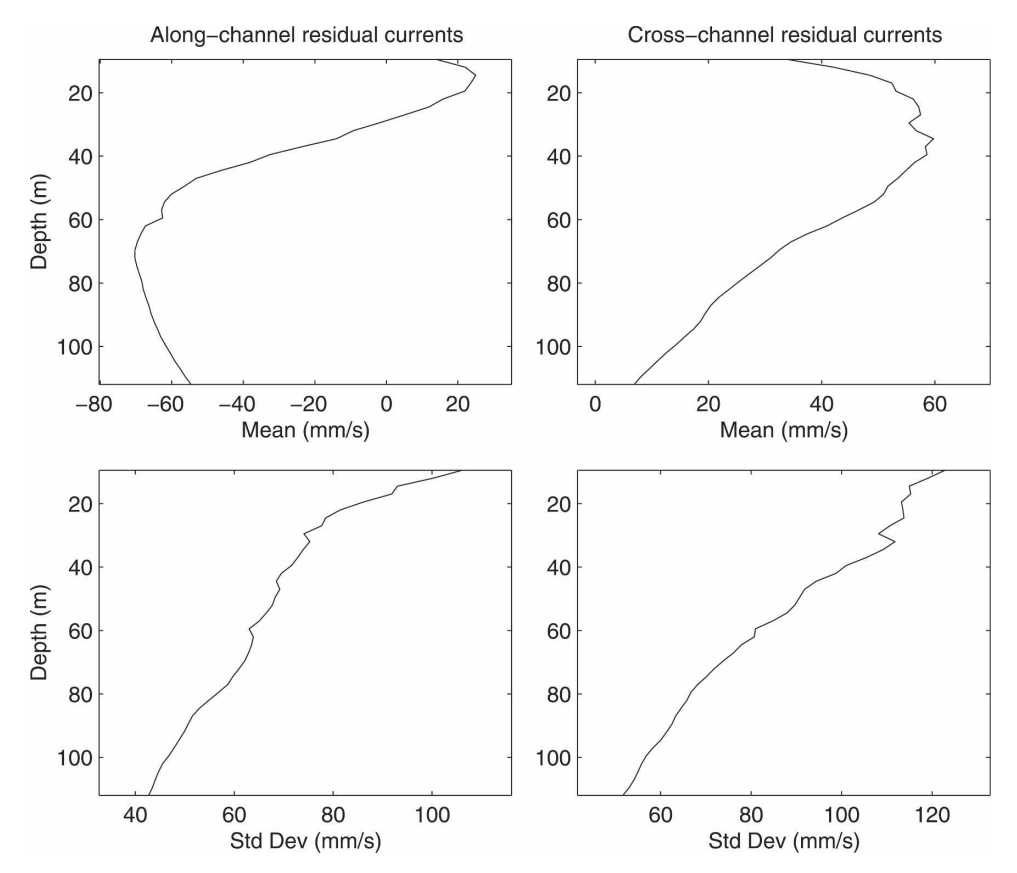


Fig. 14. (top) Mean and (bottom) standard deviation of (left) along- and (right) cross-channel residual currents in the lower St. Lawrence Estuary (mooring SLE).

The existence of a transverse current in the region of SLE in summer has been noted by several authors (El-Sabh et al. 1982; Lie and El-Sabh 1983; Mertz et al. 1989; Ingram and El-Sabh 1990). Its presence is usually associated with a stationary cyclonic eddy residing between the head of the Laurentian Channel and Rimouski and an anticyclonic eddy lying between Rimouski and Pointe-des-Monts (the opening to the gulf). This three-dimensional behavior can be understood in terms of the moderately high Kelvin number of the estuary. The Kelvin number (Garvine 1986) is the ratio of the width of the estuary to the internal deformation radius. Here, the deformation radius is roughly 10 km (Mertz et al. 1988), and thus the Kelvin number is in the range of 3–5. For estuaries with a high Kelvin number, the Coriolis force is dominant and the surface outflow will tend to be trapped near shore. For a moderately high Kelvin number, the presence of instabilities may allow the current to detach and interact with the opposing shore. Moreover, the current may attach to the opposing shore (Carstens et al. 1984), thus allowing a stable north shore current. Mertz et al. (1989) suggest that the residual surface currents in the estuary oscillate between two configurations—one with the usual estuarine outflow along the south coast and the second with a transverse current at Rimouski and a north shore current downstream. However, the mechanisms involved in the formation of these eddies and transverse currents are not well understood. Farquharson (1966) suggests tidal forcing may be responsible, whereas Murty and El-Sabh (1977) provide a possible explanation in terms of an internal adjustment from meteorological forcing. El-Sabh et al. (1982) also find evidence in support of an atmospheric connection. However, we find relatively low values of the correlation and coherence of the residual currents with atmospheric winds. In agreement with previous studies though, a peak in the variance of the transverse currents is found at 13 days.

b. Subtidal salinity and temperature

Strong low-frequency variability is present at HLC (Fig. 4), with a warming until March and a cooling and freshening thereafter. At NWG, a transition to colder temperatures occurs rapidly at the end of March (Fig. 5). The subtidal residual temperature for SLE also

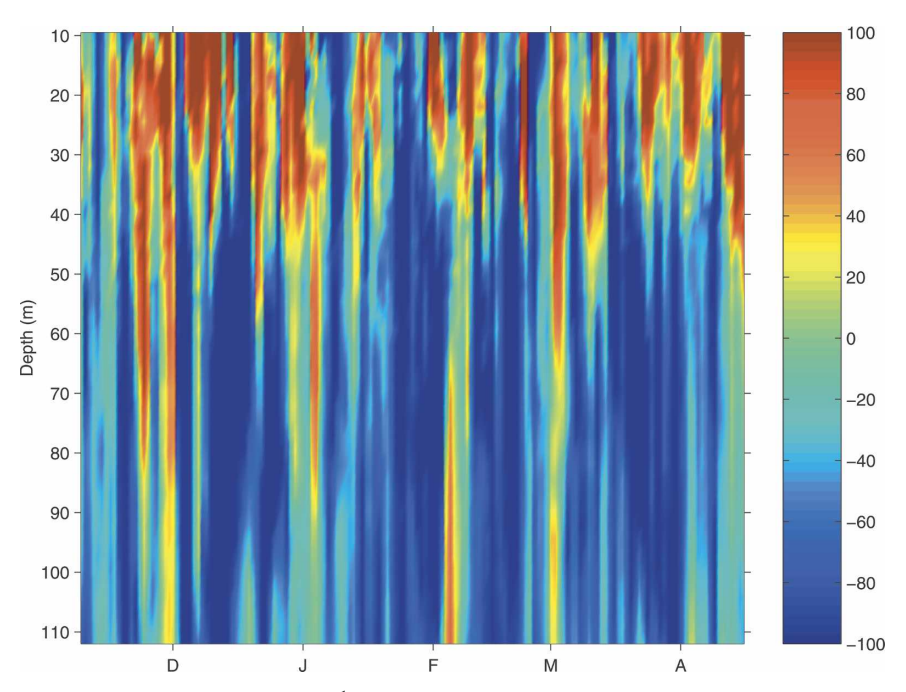


Fig. 15. Tidal residual (mm s⁻¹) of along-channel currents in the lower St. Lawrence Estuary (mooring SLE). The vertical resolution of the ADCP observations is 2.5 m.

shows a spring transition (not shown, similar to Fig. 3). As mentioned in section 2b, a shoaling of the 3°C isotherm is present from November to March. A subsequent transition to a well-defined three-layer structure

then occurs around 26 March. This transition is accompanied by a retreat of the 3°C isotherm from 80 to 160 m over the course of about two weeks. The sudden presence of a cold intermediate layer, with subzero

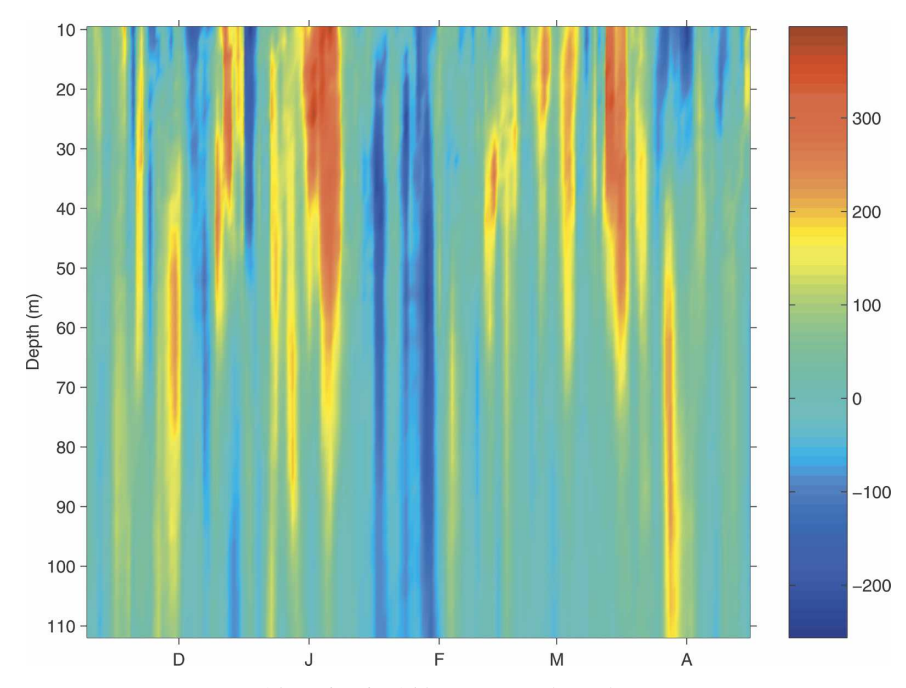


Fig. 16. As in Fig. 15 but of cross-channel currents.

temperatures at depths of 40–100 m, is most likely associated with the transport of a water mass from outside the estuary. With surface waters having begun warming in response to positive net heat fluxes from the atmosphere prior to its arrival (see Fig. 6), a local formation is unlikely.

The cold intermediate layer present in the St. Lawrence Estuary and Gulf of St. Lawrence in summer has been studied by many authors (e.g., Lauzier and Bailey 1957; Banks 1966; Bugden 1981; Gilbert and Pettigrew 1997). This layer is thought to be formed largely in situ in the gulf (Banks 1966) with inflow from the Labrador Sea through the Strait of Belle Isle contributing between 26% and 53% (Petrie et al. 1988). Ingram (1979), using data from 1973/74 at the head of the Laurentian Channel, notes that colder waters were present in spring than during winter. He also suggests that this renewal is due to upstream advection of subzero waters from the gulf. However, if the upstream advection of these waters from the gulf occurs throughout winter, one would expect to observe in Fig. 3 a gradual replenishment of the volume of this layer. The relatively short time scale (~14 days) of this renewal suggests that an external control of the flow of these cold waters may exist, perhaps by the northwest gulf. The role of the northwest gulf in controlling the timing of the renewal is addressed in a subsequent study (Smith et al. 2006).

The influx of the Atlantic layer throughout winter is consistent with the findings of Lauzier and Bailey (1957) that a shoaling of the 4°C isotherm was observed in fall. The rapid transition observed in spring, with the outflow of the bottom layer and renewal of the intermediate layer occurring contemporaneously, suggests that the estuarine circulation and deep water renewal may exhibit a strong seasonality that has not previously been observed.

6. Conclusions

a. Response to tidal forcing

The response of the St. Lawrence Estuary to tidal and atmospheric forcing in winter has been studied. A comparison of the M_2 tide from a harmonic analysis of ADCP current observations to those of Forrester (1974) in ice-free months were consistent with increased surface drag due to sea ice. The baroclinic currents at SLE confirmed the presence of a semidiurnal internal wave in winter. The depth of this wave was seen to be greater than in ice-free months, likely due to the reduced wintertime stratification. The existence of this wave in wintertime may help us to understand a previously unexplained buildup and relaxation of sea ice pressure in the estuary. These pressure variations

may be due to regions of convergence and divergence between crests and troughs of progressive semidiurnal internal tides. However, the wavelength of these waves, and hence the scale of sea ice pressure variations, will depend on the stratification of the estuary. Given that there is a weakened stratification in winter, the axial wavelength of the internal wave will be shorter than the 60 km suggested by Forrester (1974), thereby intensifying the effects on sea ice cover. However, important variations in runoff, surface forcing, and the properties of waters entering the estuary will all have an effect on this wavelength and, hence, may produce an interannual variability in the influence of the internal tides on sea ice.

A fortnightly enhancement of the estuarine circulation at neap tide was found. This oscillation may be due to mixing-induced variations in the drag between inflowing and outflowing layers. Namely, when the tidal mixing is at its minimum, the vertical turbulent fluxes of momentum are also at their minimum, effectively reducing the drag between layers. Another possibility is that fortnightly variability in freshwater discharge from the St. Lawrence River is sufficient to modulate the mixing intensity, and hence the density-driven flow. A detailed study including measurements of turbulent fluxes is required to further elucidate the dynamics of the estuarine circulation.

The harmonic analysis of thermistor data at SLE showed a 180° phase shift at fortnightly periods. In winter, the deeper layer of Atlantic waters is warmer than those above it. The phase shift is thus representative of an MS_f -modulated vertical heat flux, such that shallower waters warm and deeper waters cool during spring tide. Given that the phase shift lies below the depth of the cold intermediate layer, this suggests that the MS_f tide acts to warm this cold layer throughout winter.

b. Response to atmospheric forcing

A less significant correlation and coherence with atmospheric forcing was found than in previous studies during ice-free months. Correlation values showed a response similar to that found by Mertz et al. (1988), with flow opposite to the direction of along-channel winds. However, the correlation values at all depths were less than those of Mertz et al. (1988). Although large amplitude transverse currents were observed, we found no significant correlation or coherence with the winds. Despite the strength of the winds in winter, we did not find the strong coherence found previously for ice-free months. The limited values of the coherence squared obtained here suggest that the integrated effect

of sea ice in the estuary is to prevent momentum transfer from the atmosphere.

c. Residuals

Observations strongly suggesting a nonlocal origin for the cold intermediate layer in the St. Lawrence Estuary were presented. The abrupt renewal of this water mass in the estuary for 2003 was seen to occur in late March and was approximately 60 m thick—this observed despite mixed layer depths greater than 80 m occurring throughout most regions of the gulf by February. Given that inflow at these depths occurred throughout most of the winter at SLE, the sudden presence of this layer suggests that a change occurred in the water masses at the mouth of the estuary in the northwest gulf.

An influx of the deep Atlantic layer throughout winter was observed. A rapid transition occurred in spring, with the outflow of the bottom layer and renewal of the cold intermediate layer occurring contemporaneously. This suggests that the estuarine circulation and deepwater renewal may exhibit a strong seasonality that has not previously been observed.

A strong transverse current in the estuary was detected with a greater amplitude than the residual along-channel flow. This highlights the important three-dimensionality of the St. Lawrence Estuary and suggests that the transverse component may be responsible for providing a larger component of the surface estuarine outflow than the along-channel flow. Certainly, any estimate of the estuarine circulation intensity must take into account the transverse component.

Acknowledgments. This work has been funded by the Canadian CLIVAR network, Fisheries and Oceans Canada as well as by an NSERC scholarship to G.C.S. We thank Alain Gagné, Rémi Desmarais, Sylvain Cantin, and Roger Pigeon for their technical assistance with the moorings. We appreciate the help of Simon Senneville in obtaining the Minilog data. We are grateful to the captain and crew of the C.C.G.S. Martha Black for their assistance in the deployment and retrieval of the moorings. The MATLAB scripts created by Zhigang Xu (tidal ellipse conversion) and Rich Pawlowicz and colleagues [T_tide; Pawlowicz et al. (2002)] were quite helpful. Thanks are given to two anonymous reviewers for their helpful comments.

REFERENCES

Baker, P., and S. Pond, 1995: The low-frequency residual circulation in Knight Inlet, British Columbia. J. Phys. Oceanogr., 25, 747–763.

- Banks, R. E., 1966: The cold intermediate layer of the Gulf of St. Lawrence. *J. Geophys. Res.*, **71**, 1603–1610.
- Bugden, G. L., 1981: Salt and heat budgets for the Gulf of St. Lawrence. *Can. J. Fish. Aquat. Sci.*, **38**, 1153–1167.
- Carstens, T., T. A. McClimans, and J. H. Nilsen, 1984: Satellite imagery of boundary currents. *Remote Sensing of Shelf Sea Hydrodynamics*, J. Nilsen, Ed., Elsevier, 235–256.
- Dawson, W. B., 1901: The currents in the Gulf of St. Lawrence. *Nature*, **63**, 311–313.
- El-Sabh, M. I., H. J. Lie, and V. G. Koutitonsky, 1982: Variability of the near-surface residual current in the lower St. Lawrence Estuary. *J. Geophys. Res.*, **87**, 9589–9600.
- Farquharson, W. I., 1966: St. Lawrence Estuary current surveys. Bedford Institute of Oceanography Rep. BIO 66-6, 84 pp.
- —, 1970: Tides, tidal streams and currents in the Gulf of St. Lawrence. Bedford Institute of Oceanography AOL Rep. 1970-5, 145 pp.
- Foreman, M. G. G., 1977: Manual for tidal heights analysis and prediction. Institute of Ocean Sciences Pacific Marine Science Rep. 77-10, 58 pp.
- Forrester, W. D., 1972: Internal tides in the St. Lawrence Estuary. *Int. Hydrol. Rev.*, **49**, 55–65.
- —, 1974: Internal tides in the St. Lawrence Estuary. *J. Mar. Res.*, **32**, 55–65.
- Garvine, R. W., 1986: The role of brackish plumes in open shelf waters. The Role of Freshwater Outflow in Coastal Marine Ecosystems, S. Skreslet, Ed., Springer-Verlag, 47–65.
- Geyer, W. R., and G. A. Cannon, 1982: Sill related processes related to deep water renewal in a fjord. *J. Geophys. Res.*, **87** (C10), 7985–7996.
- Gilbert, D., and B. Pettigrew, 1997: Interannual variability (1948–1994) of the CIL core temperature in the Gulf of St. Lawrence. *Can. J. Fish. Aquat. Sci.*, **54**, 57–67.
- Godin, G., 1972: *The Analysis of Tides*. University of Toronto Press, 264 pp.
- Gratton, Y., G. Mertz, and J. Gagné, 1988: Satellite observations of tidal upwelling and mixing in the St. Lawrence Estuary. J. Geophys. Res., 93 (C6), 6947–6954.
- Hibiya, T., and P. H. LeBlond, 1993: The control of fjord circulation by fortnightly modulation of tidal mixing processes. *J. Phys. Oceanogr.*, **23**, 2042–2052.
- Ingram, G. R., and M. I. El-Sabh, 1990: Fronts and mesoscale features in the St. Lawrence Estuary. *Oceanography of a Large-Scale Estuarine System: The St. Lawrence*, M. I. El-Sabh and N. Silverberg, Eds., Springer-Verlag, 71–93.
- Ingram, R. G., 1979: Water mass modification in the St. Lawrence Estuary. *Nat. Can.*, **106**, 45–54.
- Johannesson, O. M., E. R. Pounder, H. Serson, J. Keys, D. Lindsay, W. Seifert, and E. Banke, 1968: Preliminary report on the "Ice Drift Study" in the Gulf of St. Lawrence, Winter 1968.
 McGill University Marine Science Center Marine Science Rep. 4, 21 pp.
- Koutitonsky, V. G., and G. L. Bugden, 1991: The physical oceanography of the Gulf of St. Lawrence: A review with emphasis on the synoptic variability of the motion. *The Gulf of St. Lawrence: Small Ocean or Big Estuary?* Vol. 113, J.-C. Therriault, Ed., Canadian Special Publication of Fisheries and Aquatic Science, 57–90.
- Lauzier, L. M., and W. B. Bailey, 1957: Features of the deep waters of the Gulf of St. Lawrence. *Bull. Fish. Res. Board Can.*, 111, 213–250.
- LeBlond, P., 1989: Forced fortnightly tides in shallow rivers. Atmos.—Ocean, 17, 253–264.

- ——, H. Ma, F. Doherty, and S. Pond, 1991: Deep and intermediate water replacement in the Strait of Georgia. *Atmos.—Ocean*, 29, 288–312.
- Lie, H. J., and M. I. El-Sabh, 1983: Formation of eddies and transverse currents in a two-layer channel of variable bottom with application to the lower St. Lawrence Estuary. *J. Phys. Oceanogr.*, **13**, 1063–1075.
- Matheson, K. M., 1967: The meteorological effect on ice in the Gulf of St. Lawrence. McGill University Marine Science Center Marine Science Rep. 3, 110 pp.
- Mertz, G., M. I. El-Sabh, and V. Koutitonsky, 1988: Wind-driven motions at the mouth of the lower St. Lawrence Estuary. *Atmos.-Ocean*, 26, 509–523.
- —, —, and V. G. Koutitonsky, 1989: Low frequency variability in the lower St. Lawrence Estuary. J. Mar. Res., 47, 285–302.
- Murty, T. S., and M. I. El-Sabh, 1977: Transverse currents in the St. Lawrence Estuary: A theoretical treatment. *Transport Processes in Lakes and Oceans*, R. J. Gibbs, Ed., Plenum, 25–62.

- Pawlowicz, R., B. Beardsley, and S. Lentz, 2002: Classical tidal harmonic analysis including error estimates in MATLAB using T_TIDE. Comput. Geosci., 28, 929–937.
- Petrie, B., B. Toulany, and C. Garrett, 1988: The transport of water, heat and salt through the Strait of Belle Isle. *Atmos.—Ocean*, **26**, 234–251.
- Saucier, F. J., and J. Chassé, 2000: Tidal circulation and buoyancy effects in the St. Lawrence Estuary. Atmos.—Ocean, 38, 505– 556
- Smith, G. C., F. J. Saucier, and D. Straub, 2006: Formation and circulation of the cold intermediate layer in the Gulf of Saint Lawrence. J. Geophys. Res., 111, C06011, doi:10.1029/ 2005JC003017.
- Stacey, M. W., S. Pond, P. H. LeBlond, H. J. Freeland, and D. M. Farmer, 1987: An analysis of the low-frequency current fluctuations in the Strait of Georgia, from June 1984 until January 1985. J. Phys. Oceanogr., 17, 326–342.
- Tee, K.-T., 1989: Subtidal salinity and velocity variations in the St. Lawrence Estuary. *J. Geophys. Res.*, **94** (C6), 8075–8090.